A Semiautomated Electron Backscatter Diffraction Technique for Extracting Reliable Twin Statistics

B.L. HENRIE, T.A. MASON, and B.L. HANSEN

A framework has been developed for extracting reliable twin statistics from a deformed microstructure using crystallographic twin identification techniques with spatially correlated electron backscatter diffraction (EBSD) data. The key features of this analysis are the use of the mathematical definition of twin relationships, the inclination of the common K_1 plane at a twin boundary, and the correct identification of the parent orientation in a parent/twin pair. Methods for identifying the parent in a parent/twin pair will be briefly discussed and compared. Twin area fractions are then categorized by operative twin systems, number of active twin variants in each system, and corrected twin widths. These statistics are reported here for α-zirconium samples deformed in quasi-static four-point bend beams and in a 100 m/s Taylor cylinder impact test. Analysis of the statistics also begins to reveal the roles that deformation rate and relative orientation of the boundary conditions to the material's symmetry axes play in determining the twinning activity that accommodates the imposed boundary conditions. These improved twin statistics can help quantify the deformation processes in materials that deform by twinning as well as serve to provide better validation of proposed models of the deformation processes.

I. INTRODUCTION

DEFORMATION twinning is an important mechanism in the plastic response of many materials[1,2] and theories that attempt to capture twinning activity have begun to be incorporated into deformation modeling efforts.[3,4] As the predictive capabilities of twin models improve, gross measures of twin density or twin area fractions may no longer be sufficient validation metrics. Details of the microscopic deformation such as the balance between competing twin types, the number of active twin variants for each twin type, and characterization of twin morphology may be required to validate deformation models. One example of this progression toward the need for greater microstructural detail can be seen in studies of shape memory alloys.[5,6] The authors have developed a technique to quantify the amount of twinning in a material according to categories such as twin type, number of twin variants, twin thickness, and geometry. This technique allows the influence of initial or boundary conditions such as strain, strain rate, and temperature on twin activity to be quantified.

A search of the literature regarding twin activity does yield reports of twinning as functions of strain, strain rate, temperature, and grain size.[1,2,7–21] These reports were generated using a combination of four processes: optical microscopy, transmission electron microscopy (TEM), neutron diffraction, and automated electron backscatter diffraction (ESBD). Optical microscopy can only identify probable twins using grain shape as the sole criteria. Mahajan *et al*.[12] show several twin shapes for face-centered-cubic crystals. Optical analysis cannot distinguish between twin types or twin variants, or provide any information regarding the probable true thickness of the identified twins without resorting to serial sectioning. At low strains, twins are usually easily identified by their morphologies if the sample has been properly etched. However, as the twin density increases, it often becomes more difficult to differentiate between parent grains and deformation twins by their morphology alone. Several authors do report twin densities or area fractions,[10–21] while others only reported general comments such as "low in density" or "high in density".[7,8,9] The major limitation of this process is the reliance on visual inspection of twin boundaries without the aid of crystallographic information.

The TEM studies can yield detailed crystallographic information about individual twins or small numbers of twins. But the labor intensive nature of this technique precludes producing sufficient statistical data for model validation. To obtain more statistical information, optical microscopy has been applied in conjunction with TEM, but again, the reported results only included twin area fractions.[16,17,18]

The application of neutron diffraction data has the advantage that volume fractions of twins can be determined based on assumptions regarding active twin modes, but twin morphology and the number of active twin variants are not accessible.[20,21] Additionally, small differences between the volume fractions of competing twin modes may not be recognized due to the nature of the diffraction measurement and analysis. The obvious major restriction on the use of neutron texture measurements to identify twinning fractions is the limited access to a neutron source with the proper detectors.

Automated EBSD can produce large numbers of spatially correlated measurements of crystallographic orientation.[22] Analysis of these data sets can enable the quantification of twinning with greater accuracy than is available through optical microscopy[23–26] and yield better statistical data than TEM. To expand on this capability, a semiautomated analysis technique was developed that first identifies and verifies possible twin boundaries in a deformed microstructure using the proposed criterion[23] and then associates these twin boundaries with manually preselected parent orientations in each

B.L. HENRIE and T.A. MASON, Technical Staff Members, are with Los Alamos National Laboratory, Los Alamos, NM 87545. Contact e-mail: henrie@lanl.gov B.L. HANSEN, Doctorate Student, is with the Division of Engineering and Applied Science, California Institute of Technology, Pasadena, CA 911285.

Manuscript submitted February 2, 2004.

grain. This association of parent orientation and verified twin boundaries allows the twin interiors to be differentiated from the original parent grains. Once the deformation twins in a microstructure are correctly identified, the twin fractions can be categorized by considering details such as active twin systems, number of twin variants present, twin widths, and other correlations to the loading conditions.

II. MATERIAL

The α-zirconium samples were obtained from clock-rolled and fully recrystallized crystal-bar plate. The chemistry was O $<$ 50, C $<$ 22, N $<$ 50, Fe $<$ 50, Al $<$ 20, V $<$ 50, Hf $<$ 35, and Ti $<$ 25 ppm. The original microstructure consisted of equiaxed grains with a mean grain size of 25 μm. Bingert *et al.*[24] reported the initial material to be devoid of twins with a relatively strong axisymmetric $<0001>$ crystallographic texture aligned normal to the plate.

The α-zirconium was deformed following two different paths: a quasi-static, four-point bend beam experiment[27] and a 100 m/s Taylor cylinder impact test.[28] The bend beam experiment subjected the top and bottom fibers of a prismatic beam sample to compressive and tensile stresses, respectively. Two sample orientations were tested in the bend beam experiments: "0" corresponding to the plate normal being vertical and "90" corresponding to the plate normal being horizontal.

In a Taylor cylinder impact test, a metal cylinder is launched against a rigid anvil at high speed. As the cylinder impacts the anvil, sequential layers of material deform as a compressive stress wave travels up the cylinder axis. Due to the nature of the anisotropic, in-plane strain hardening of this zirconium and the relatively modest impact velocity, the first 14 mm of the cylinder experienced a nearly uniform strain of approximately 0.20.

III. PROCEDURE

A semiautomated technique was developed to use manual parent orientation selection with an automated routine that identifies twin boundaries that are consistent with all available crystallographic data. The initial task in quantifying twin areas or volumes is to determine which areas in a deformed microstructure correspond to the parent or original grains. Each parent orientation is recorded for use in an automated program, as explained subsequently.

Other schemes of parent selection have been presented in the literature. Bingert *et al.*[24] reported that the operative twin variants in twinned grains were not always the twin variant with the maximum resolved shear stress or Schmid factor. This led them to conclude that the sole use of the Schmid factor for parent determination could render incorrect analysis. The deficiency in this analysis arises from the use of a known, "uniform" macroscopic stress instead of the actual, unknown local stress field to calculate the resolved shear stress. Another scheme using a "majority rule" selection criterion[26] has been proposed that assumes that the area of twinned material will be less than one-half of the original volume; thus, the dominant orientation within a grain is assumed to be the parent orientation. This approach has the advantage that the twin calculations can be completely automated in a straightforward manner. However, this approach suffers from the limitation that at large strain, the parent orientation is frequently not the majority orientation. A comparison between manual parent selection and majority rule schemes will be reported later in this article.

With the parent orientations having been selected manually, mathematical analysis of the crystal orientations can be used to probe local changes in the lattice orientations and determine their consistency with twin characteristics. Mason *et al.*[23] suggested three criteria for verifying that any given grain boundary was most likely a twin boundary. The first criterion for twin boundary identification is that the relative misorientation between two lattice points be consistent with a twin definition. Table I shows the twin definitions for α-zirconium. A misorientation angle tolerance of ± 5 deg was used. This criterion determines which twin type is likely to be present. The second criterion examines the twin/parent boundary to verify that a common crystallographic plane is present. This plane, called the K_1 plane, is shown in Table I for each twin type. For this study, an allowable misalignment of K_1 plane normals of ± 3 deg was used. This second test eliminates some orientation pairs that are related by a twin-type misorientation, but that do not share a possible twin-type interface. This criterion also determines which variant of the twin type identified in the previous step actually shares the proper K_1 plane with the parent orientation. The third criterion is simply that the predicted grain boundary should be consistent with the experimentally observed grain boundary. This third step uses the K_1 plane and determines the inclination of the twin or K_1 plane to the observed section plane of the sample. The line of intersection of the predicted twin plane and the sample section plane should be parallel to the experimental grain boundary. The details of this comparison are discussed by Wright *et al.*[26] This third criterion is called the twin boundary trace comparison. Mason *et al.*[23] provided explicit examples of these three criteria with corresponding advantages and limitations.

A baseline twin area fraction technique was developed for comparison with the semi-automated method. For this baseline technique, the misorientation, K_1 plane coincidence, twin morphology, and twin boundary trace were all individually verified for each twin occurrence. If a twin was found that met all twin criteria, then the twin interior was colored black, as shown in Figure 1(a). Figure 1(b) shows an EBSD map of the same microstructure before twin identification was performed. A pixel count was then performed to determine the twin area fraction. Since all twin criteria were individually checked, this method is believed to be very accurate. The obvious disadvantage of this method is the time required to perform the analysis of each data set. This time investment makes this method less desirable for gathering statistics from a large number of twins.

Table I. Twin-Type Parameters for α-Zirconium[29]*

Type	K_1 Plane	η_1 Direction	Misorientation	
T1	$\{10\bar{1}2\}$	$<10\bar{1}\,\bar{1}>$	$<\bar{2}110>$	-64.22 deg
T2	$\{11\bar{2}1\}$	$<11\bar{2}\bar{6}>$	$<10\bar{1}0>$	-94.78 deg
C1	$\{11\bar{2}2\}$	$<11\bar{2}\bar{3}>$	$<10\bar{1}0>$	-34.84 deg
C2	$\{10\bar{1}1\}$	$<10\bar{1}\,\bar{2}>$	$<\bar{2}110>$	-57.05 deg

*T1 is tension twin and C1 is compressive twin.

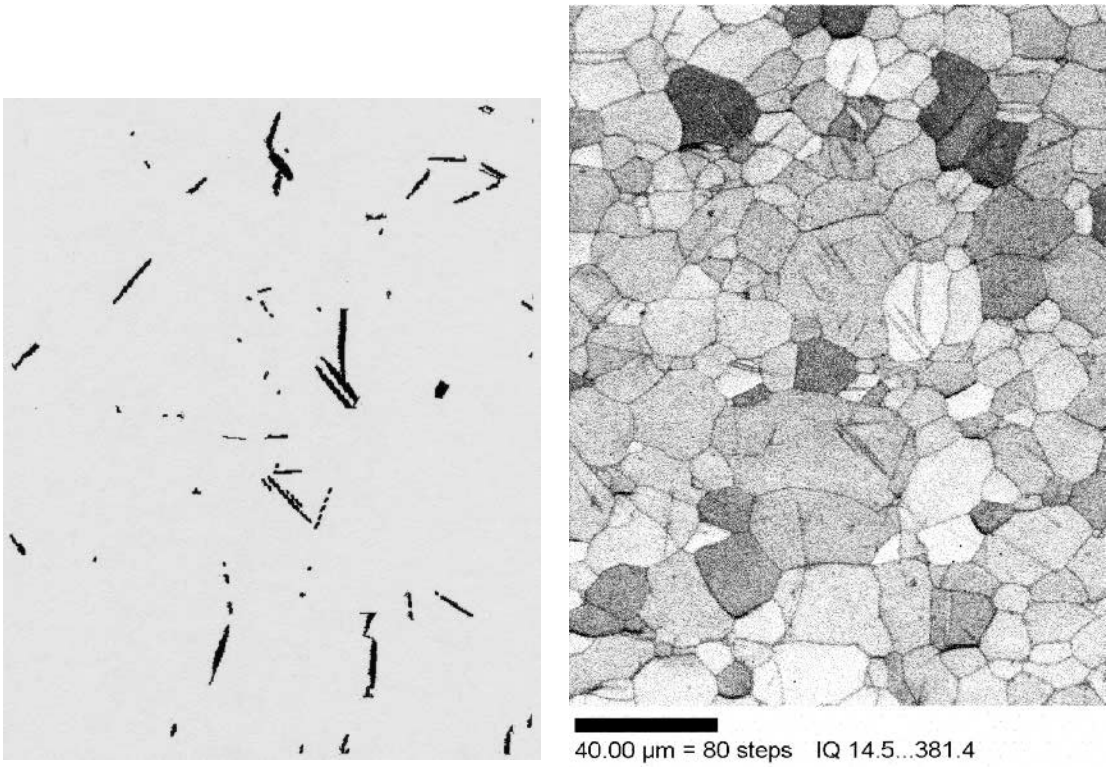

(*a*) (*b*)

Fig. 1—Four percent compressed α-Zr sample: (*a*) areas defined as twins from baseline measurement and (*b*) EBSD microstructure map.

Table II. Twin Area Fractions Comparing the Accuracy of Parent Selection Routines; Tests Were Performed on Four Compression Specimens at Different Strains

Parent Selection						
Twin Criteria Tests		Manual		Majority		
Strain	Experiment	Misorientation	K_1	Misorientation	Trace	Baseline
4 pct	bent beam	4.4 pct	4.3 pct	5.1 pct	4.5 pct	4.3 pct
4 pct	Taylor	1.4 pct	1.4 pct	2.4 pct	1.7 pct	1.2 pct
6 pct	Taylor	9.1 pct	9.0 pct	12.6 pct	8.6 pct	10.2 pct
14 pct	Taylor	12.6 pct	12.5 pct	18.4 pct	15.8 pct	12.1 pct

IV. RESULTS

Four test analyses were performed to determine how the accuracy of the twin identification process was affected by the choice of the parent selection method. For the first test, the misorientation criterion was performed with manually selected parent orientations. In the second test, the K_1 coincidence criterion was used with manual parent selection. For the third test, the misorientation criterion was used with the majority rule. Last, the fourth test employed the grain boundary trace with the majority rule. Table II reports the results of the four tests and the baseline measurements for four deformed samples.

By plotting the error between the baseline measurements and each of the four tests, it is evident that as the plastic strain level increases, the disparity between the majority rule and manual selection process increases, as shown in Figure 2. Although the manual parent selection method is more time intensive than the majority rule method, the manual

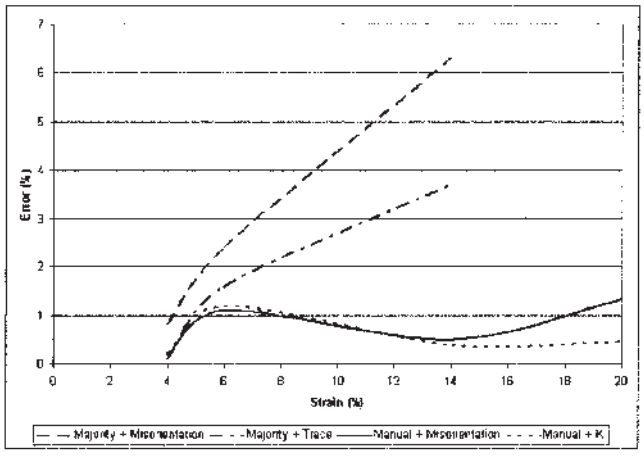

Fig. 2—Error between the baseline and the two parent selection routines for the Taylor cylinder experiments.

method produces consistently lower errors. Figure 2 also shows that at strains greater than about 16 pct, the misorientation with manual parent selection method breaks down.

Once it was determined that using manual parent selection yielded better results than the majority rule method, two additional tests were performed to identify which crystallographic twin criteria should be used for twin identification. The most correct twin data would be achieved by using all three twin criteria in sequence. However, Wright *et al.*[26] have reported that difficulties exist with the grain boundary trace criterion, so in this study, only the misorientation and K_1 plane coincidence criteria were tested in combination with manual parent selection. Table III shows the results of these tests compared with the baseline analysis. When only the misorientation criterion was used, there was an average error of 1.2 pct from the baseline area fractions. When both the misorientation and the K_1 plane coincidence criterion are combined, the average error dropped to 0.75 pct. From these results, the authors believe that the combined use of the misorientation and K_1 plane criteria are sufficient for the majority of twin area fraction determinations, without incurring the operational penalties involved in finding the boundary trace.

The misorientation and K_1 plane criteria with manual parent selection were applied to both the Taylor and bend beam experiment. Tables IV and V contain the results of this analysis. Note that the locations called out in Table IV are with respect to the impact interface.

As was stated previously, the K_1 plane can be used to identify which twin variants are active in each twin system. Figures 3 and 4 report the variant results for both the Taylor cylinder and bent beam experiments.

Another metric that can be applied to help understand deformation twinning is to compute the effective grain size of the material. Twin boundaries are assumed to inhibit dislocation motion and are calculated as separate grains. This is shown in Table VI. The original grain size was 25 μm.

Table III. Improved Accuracy is Gained by Incorporating Multiple Twin Criterions*

Twin Criteria Tests				
Strain	Experiment	Misorientation	K_1	Baseline
4 pct C	bent beam	4.4 pct	4.3 pct	4.3 pct
10 pct C	bent beam	19.1 pct	19.0 pct	20.5 pct
16 pct T	bent beam	4.3 pct	4.1 pct	4.9 pct
4 pct C	Taylor	1.4 pct	1.4 pct	1.6 pct
6 pct C	Taylor	9.1 pct	9.5 pct	10.2 pct
14 pct C	Taylor	12.6 pct	11.3 pct	12.1 pct
20 pct C	Taylor	44.7 pct	41.5 pct	42.0 pct

*C denotes compressive stress, and "T" denotes tensile stress.

V. DISCUSSION

An accurate technique for twin identification has been developed that produces quantified twin area fractions with distinctions made as to twin type and the number of active variants. This is a significant step beyond the best results derived from metallographic examinations as optical techniques cannot access the crystallographic information that defines twin types. The active twin systems and number of variants, corrected twin widths, and effective grain sizes present in the deformed α-zirconium samples were analyzed for both types of experiments and are reported in section IV. This additional twin information adds statistical insight into deformation behavior that was previously only accessible by TEM studies.

Examination of the twin area fraction results for the Taylor cylinder reported in Table IV reveals that while the fraction of {1012} twins present in this first 11 mm was roughly constant at around 0.30, the fraction of {1121} twins decreased from about 0.08 at the impact interface to 0.006 at 11 mm. It appears that the fraction of the {1122} compression twin also decreases with distance from the impact interface, but the trend is less well established. Beyond the 11-mm mark, all three twin fractions decrease with further distance from the impact interface. On average, the {1012} twin represented 86 pct of the twins in the Taylor cylinder material. The only

Table IV. Twin Area Fractions by Twin System for the 100 m/s Taylor Cylinder

Location (Strain)	36 mm (4.4 pct)	35 mm (6 pct)	30 mm (14 pct)	14 mm (21 pct)	11 mm (21 pct)	8 mm (21 pct)	4 mm (21 pct)	2 mm (21 pct)
Twin System								
$\{11\bar{2}1\}$	0.06 pct	0.17 pct	0.44 pct	0.56 pct	0.62 pct	0.82 pct	1.75 pct	7.96 pct
$\{11\bar{2}2\}$	0.11 pct	0.43 pct	1.48 pct	2.25 pct	2.80 pct	2.84 pct	1.62 pct	5.01 pct
$\{10\bar{1}2\}$	1.23 pct	8.90 pct	9.38 pct	20.02 pct	30.76 pct	27.04 pct	31.00 pct	28.53 pct
Total	1.40 pct	9.50 pct	11.30 pct	22.83 pct	34.18 pct	30.70 pct	34.37 pct	41.50 pct

Table V. Twin Area Fractions by Twin System for Bend Beam*

Temperature	77 K				298 K			
Orientation	90_C	90_T	0_C	0_T	90_C	90_T	0_C	0_T
Twin System								
$\{11\bar{2}1\}$	2.06 pct	0.08 pct	0.29 pct	0.16 pct	0.06 pct	0.22 pct	3.74 pct	0.82 pct
$\{11\bar{2}2\}$	1.27 pct	0.65 pct	1.07 pct	0.00 pct	0.65 pct	0.17 pct	0.39 pct	1.36 pct
$\{10\bar{1}2\}$	14.99 pct	4.53 pct	9.26 pct	0.95 pct	4.53 pct	3.38 pct	18.97 pct	2.35 pct
Total	18.32 pct	5.26 pct	10.62 pct	1.11 pct	5.26 pct	3.77 pct	23.10 pct	4.53 pct

*Loading sense denoted by "C" (compression) or "T" (tension). Each test experienced approximately 20 pct strain in the outermost fibers.

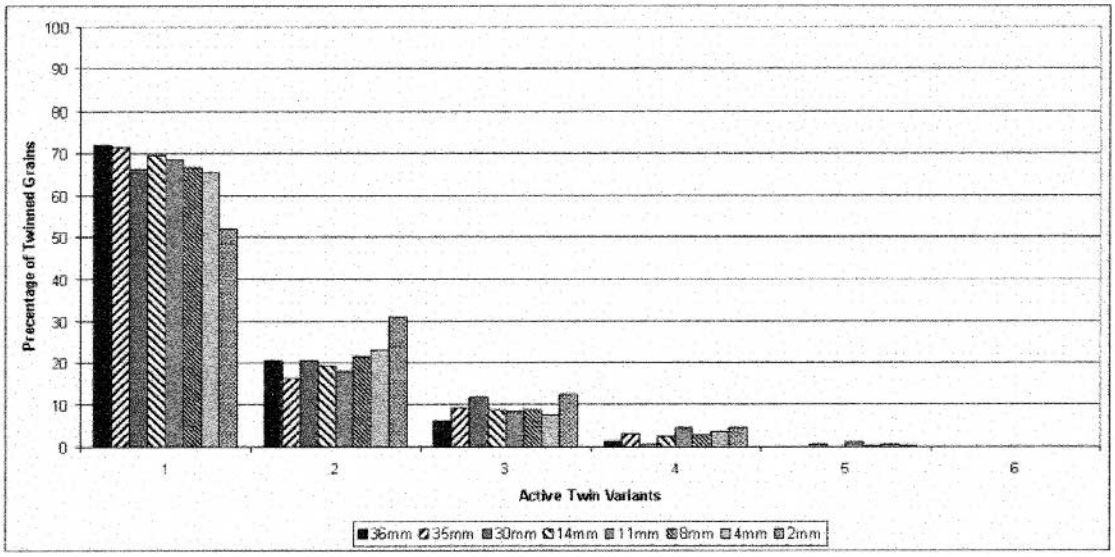

Fig. 3—Frequency of active twin variants per twinned grain in a 100 m/s zirconium Taylor cylinder.

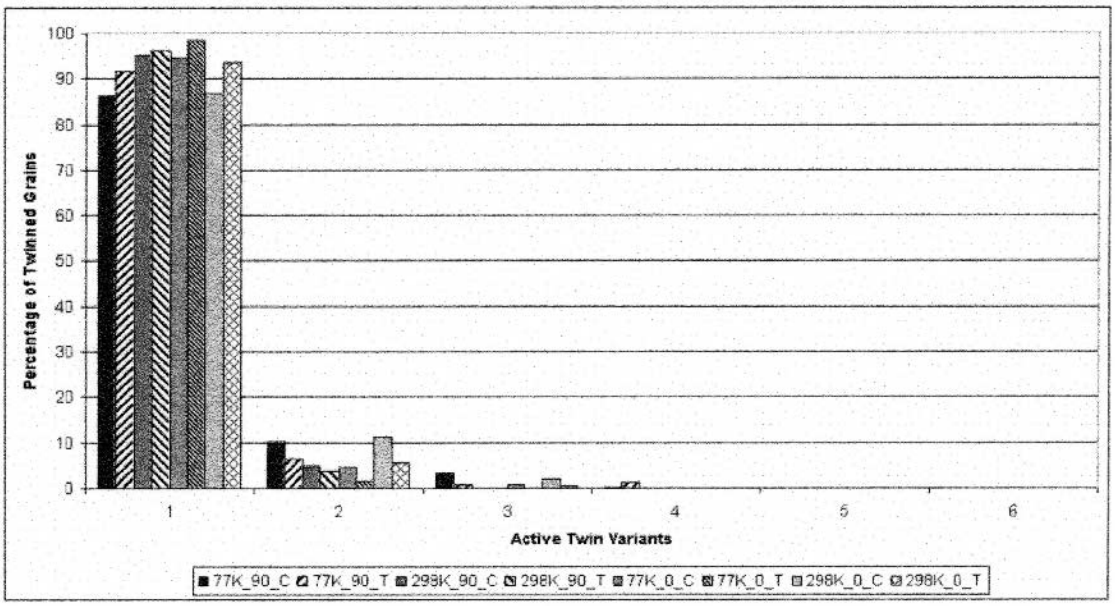

Fig. 4—Frequency of active twin variants per twinned grain in the bend beam experiment. Loading sense denoted by "C" (compression) or "T" (tension).

Table VI. Effective Grain Size Diameter by Fitting a Circle to the Grain

100 m/s Taylor Cylinder								
Location (Strain)	36 mm (4.4 pct)	35 mm (6 pct)	30 mm (14 pct)	14 mm (21 pct)	11 mm (21 pct)	8 mm (21 pct)	4 mm (21 pct)	2 mm (21 pct)
Grain size diameter (μm)	19.3	13.9	12.7	11.5	9.6	10.6	8.8	7.8
Quasi-Static four-Point Bend Beam								
Temperature	77 K				298 K			
Orientation	90_C	90_T	0_C	0_T	90_C	90_T	0_C	0_T
Grain size diameter (μm)	14.8	18.8	18.3	18.1	23.6	20.1	16.3	17.7

significant deviation from this trend was near the impact interface where a population of {1121} twins was seen.

Twin analysis results from the quasi-static, four-point bend beam experiments are reported in Table V. Again, the {1012} twin system dominated the twin area fraction statistics. Regardless of sample orientation, 0 or 90, the compression side or top of the bend beams consistently exhibited more twin activity than the tension side of the beams. The single inconsistency in this trend was reported for the {1122} twin system at room temperature and 0 orientation. In this test, the material was oriented such that the {1122} compression twin was preferentially activated on the tension side of the beam.

The strain rate dependence of twin activity can be explored when the corrected twin widths in the two types of experiments are compared. Corrected twin widths are found by using the inclination angle of the K_1 plane to find the true dimension of the projected twin width. This is shown schematically in Figure 5.

In the Taylor cylinder experiments, the twins exhibited a gradual thickening from 0.8 to 1.4 μm with increasing plastic strain. In the bend beam experiments, the corrected twin widths varied from 0.7 to 2.2 μm with a standard deviation of 1.2 μm. For the bend beam experiments, no clear trend was observed to explain the twin width variability. It was also found that the Taylor cylinder specimen had an increase in the number of active twin variants present in twinned grains. This distribution for the Taylor cylinder is shown in Figure 4, while the results for the bend beams are shown in Figure 5. In the bend beams, few grains exhibited more than a single active twin variant and the distribution appears to be independent of strain magnitude. In the Taylor cylinder, material at 2 mm from the impact interface that has experienced moderate strain and higher strain rates exhibits more active twin variants than material with the same approximate strain level but lower strain rates. Clearly, strain rate plays a role in the number of activated twin variants per grain as well as the final widths of the twins.

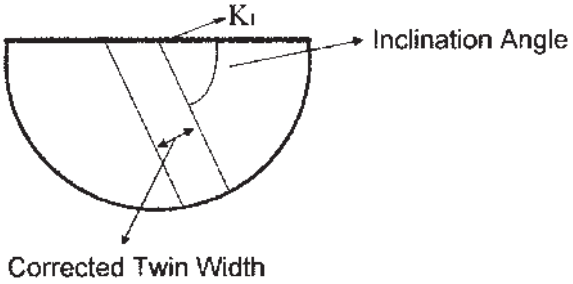

Fig. 5—Corrected twin width was computed from the inclination of the K_1 plane.

In these zirconium samples, three major twin morphologies or arrangement schemes were observed. First, sets of parallel twins of a single variant of a twin system spanning a grain, as seen in Figure 6(a), will be termed "type A." "Type B" corresponds to the presence of multiple twin variants of a single twin system creating a crisscrossing pattern similar to that shown in Figure 6(b). A microstructure with "type C" morphology exhibits multiple twin variants of multiple twin systems within a single grain, as demonstrated in Figure 6(c).

Table VI reports the average or effective grain sizes for each of the deformed microstructures in this study. The effective grain size was found by assuming that twin boundaries were grain boundaries. The Taylor cylinder showed the greatest grain size reduction from 19.3 μm at 36 mm to 7.8 μm at 2 mm. In the bend beam experiments, the effective grain size remained around 18 μm. The 77 K_0_C bend beam and the 30-mm Taylor cylinder data sets produced similar twinning statistics with a twin area fraction of about 0.11, but with effective grain sizes of 18.3 and 12.7 μm, respectively. Observations showed that the predominate grain morphology in the bend beam experiments was of type A. The microstructures in the Taylor cylinder mainly exhibited a type B morphology with an increase in type C near the impact interface. The inference made here is that at higher strain rates, more variants of more twin types are being activated than at lower strain rates.

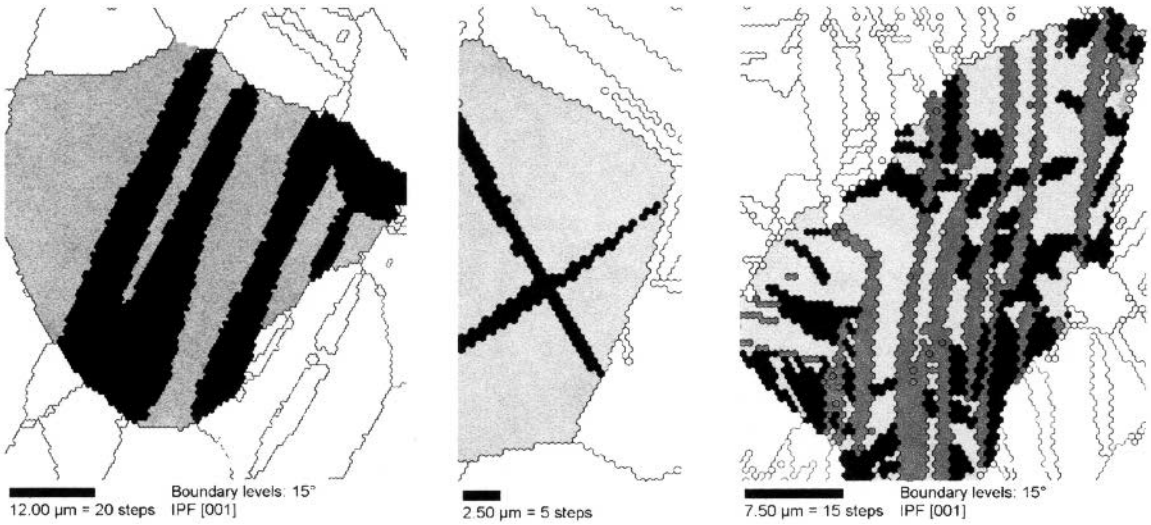

Fig. 6—Observed twin morphologies. (*a*) Parallel twins (colored black) of the $\{10\bar{1}2\}$ twin system. (*b*) Two twin variants (colored black) of the $\{10\bar{1}2\}$ twin system. (*c*) Multiple twin variants of the $\{10\bar{1}2\}$twins (colored black) and$\{11\bar{2}1\}$wins (colored dark gray) within a grain.

VI. CONCLUSIONS

As the numerical simulation of deformation of polycrystalline materials continually improves, it will become more necessary to quantify the details of complex deformation processes. Up to the present, little statistical information regarding twin activity in deformed metals was available. The present authors have developed an accurate EBSD technique for twin analysis that produces quantified statistics on twin types, active twin variants, and corrected twin widths. This is a significant step beyond the best results derived from metallographic examinations, because optical techniques cannot access the crystallographic information that defines twin types.

Manual parent selection adds a robust and efficient method of extracting twin statistics for highly strained samples where the microstructure is very complex. The combination of the misorientation and the K_1 plane criteria for twin boundary verification was found to be sufficient for the majority of twin boundaries encountered in this study.

Multiple twin systems were active in the zirconium samples tested in both the bend beam and Taylor cylinder experiments, but the higher strain rate in the Taylor cylinder activated more twin types and multiple twin variants. This additional twin information adds statistical insight into deformation behavior that was previously only accessible by TEM studies.

REFERENCES

1. J.W. Christian and S. Mahajan: *Progr. Mater. Sci*., 1995, vol. 39, p. 1.
2. M.V. Klassen-Neklyudova: *Mechanical Twinning of Crystals*, Consultants Bureau, New York, NY, 1964.
3. C.N. Tomé, P.J. Maudlin, R.A. Lebensohm, and G.C. Kaschner: *Acta Mater*., 2001, vol. 49, pp. 3085-96.
4. S.R. Kalidindi: *J. Mech. Phys. Solids*, 1998, vol. 46, pp. 267-90.
5. X.Y. Zhang, L.C. Brinson, and Q.P. Sun: *Smart Mater. Struct*., 2000, vol. 9, pp. 571-81.
6. X. Gao, M. Huang, and L.C. Brinson: *Int. J. Plasticity*, 2000, vol. 16, pp. 1345-69.
7. P.H. Adler, G.B. Olson, and W.S. Owen: *Metall. Trans. A,* 1986, vol. 17A, pp. 1725-37.
8. M.H. Yoo and C.L. Fu: *Metall. Mater. Trans. A,* 1998, vol. 29A, pp. 49-63.
9. D.H. Shin, I. Kim, J. Kim, and Y.T. Zhu: *Mater. Sci. Eng*., 2002, vol. A334, p. 239.
10. F.D. Rosi, C.A. Dube, and B.H. Alexander: *J. Met*., 1953, Feb., pp. 257-65.
11. R.N. Wright and D.E. Mikkola: *Metall. Trans. A*, 1985, vol. 16A, pp. 881-90.
12. S. Mahajan, C.S. Pande, M.A. Iman, and B.B. Rath: *Acta Metall*., 1997, vol. 45, p. 2633.
13. S.R. Kalidindi: *J. Mech. Phys. Solids*, 1998, vol. 46, pp. 267-90.
14. E. El-Danaf, S.R. Kalidindi, and R.D. Doherty: *Metall. Mater. Trans. A*, 1999, vol. 30A, pp. 1223-33.
15. M.A. Meyers, O. Vöhringer, and V.A. Lubarda: *Acta Mater*., 2001, vol. 49, pp. 4025-39.
16. D.R. Chichili, K.T. Ramesh, and K.J. Hemker: *Acta Mater*., 1998, vol. 46, pp. 1025-43.
17. A. Rohatagi, K.S. Vecchio, and G.T. Gray III: *Acta Mater*., 2001, vol. 49, pp. 427-38.
18. P. Klimanek and A. Potzsch: *Mater. Sci. Eng*., 2002, vol. A324, p. 145.
19. A.A. Salem, S.R. Kalidindi, and R.D. Doherty: *Scripta Mater*., 2002, vol. 46, pp. 419-23.
20. P. Rangaswamy, M.A.M. Bourke, D.W. Brown, G.C. Kaschner, R.B. Rogge, M.G. Stout, and C.N. Tome: *Metall. Mater. Trans. A,* 2002, vol. 33A, p. 757.
21. D.W. Brown, M.A.M. Bourke, P.S. Dunn, R.D. Field, M.G. Stout, and D.J. Thoma: *Metall. Mater. Trans. A,* 2001, vol. 32A, p. 2219.
22. B.L. Adams, S.I. Wright, and K. Kunze: *Metall. Trans*., 1993, vol. 24, p. 819.
23. T.A. Mason, J.F. Bingert, G.C. Kaschner, S.I. Wright, and R.J. Larsen: *Metall. Mater. Trans. A,* 2002, vol. 33A, p. 949.
24. I.F. Bingert, T.A. Mason, G.C. Kaschner, P.J. Maudlin, and G.T. Gray III: *Metall. Mater. Trans. A,* 2002, vol. 33A, p. 955.
25. S.I. Wright and R.J. Larsen: *J. Microsc*., 2002, vol. 205, p. 245.
26. S.I. Wright, J.F. Bingert, T.A. Mason, and R.I. Larsen: *Mater. Sci. Forum*, 2002, vols. 408–412, p. 511.
27. G.C. Kaschner, F.J. Bingert, C. Liu, M.L. Lovato, P.J. Maudlin, M.G. Stout, and C.N. Tome: *Acta Mater*., 2001, vol. 49, p. 3097.
28. P.J. Maudlin, G.T. Gray III, C.M. Cady, and G.C. Kaschner: *Phil. Trans. R. Soc. London A*, 1999, vol. 357, p. 1707.
29. E. Tenckhoff: *Deformation Mechanisms, Texture, and Anisotropy in Zirconium and Zircaloy*, ASTM STP 966, ASTM, Philadelphia, PA, 1988.